Article

Cell Systems

Pan-Cancer Analysis of Mutation Hotspots in Protein Domains

Graphical Abstract

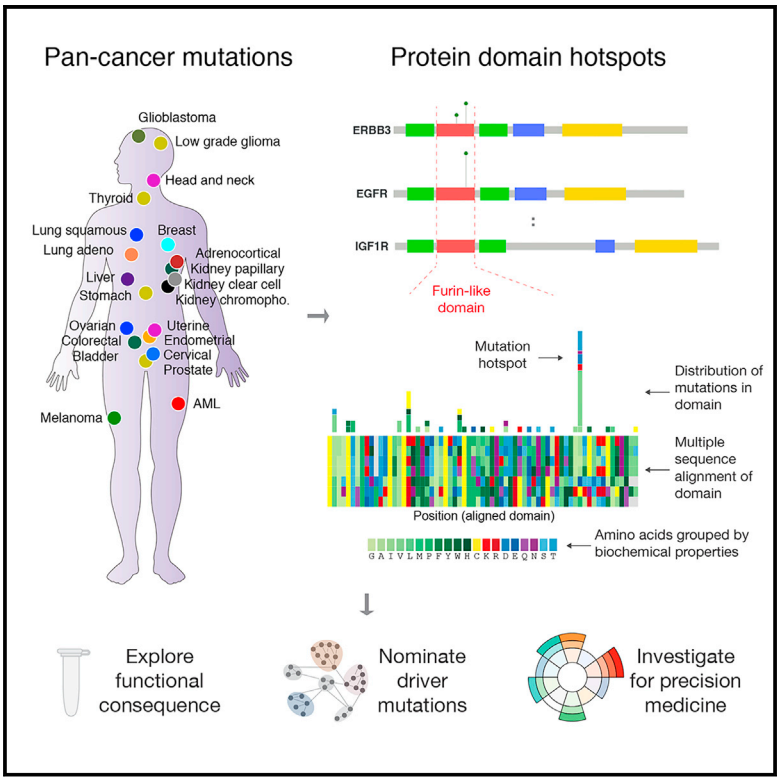

Highlights

- Comprehensive analysis of cancer mutations in protein domains (http://www.mutationaligner.org)
- Identification of new mutation hotspots across homologous domains
- Functional coupling of rare, uncharacterized mutations and known oncogenic mutations
- Mechanistic clues about downstream effects of mutations in signaling domains

Authors

Martin L. Miller, Ed Reznik, Nicholas P. Gauthier, ..., Giovanni Ciriello, Nikolaus Schultz, Chris Sander

Correspondence

mutalign@gmail.com (M.L.M.)

In Brief

Using cancer genomics datasets from thousands of tumor samples in 22 tumor types, Miller et al. analyze somatic missense mutations in protein domains and discover new domain mutation hotspots. By associating mutations in infrequently altered genes with mutations in frequently altered paralogous genes that are known to contribute to cancer, this study provides many new clues to the functional role of rare mutations in cancer.

Miller et al., 2015, Cell Systems *1*, 197–209
September 23, 2015
http://dx.doi.org/10.1016/j.cels.2015.08.014

Cell Systems
Article

Pan-Cancer Analysis of Mutation Hotspots in Protein Domains

Martin L. Miller,[1,2,*] Ed Reznik,[1] Nicholas P. Gauthier,[1] Bülent Arman Aksoy,[1] Anil Korkut,[1] Jianjiong Gao,[1] Giovanni Ciriello,[1] Nikolaus Schultz,[1] and Chris Sander[1]
[1]Computational Biology Program, Memorial Sloan Kettering Cancer Center, 1275 York Avenue, New York, NY 10065, USA
[2]Cancer Research UK Cambridge Institute, University of Cambridge, Li Ka Shing Centre, Robinson Way, Cambridge CB2 0RE, UK
*Correspondence: mutalign@gmail.com (M.L.M.)
http://dx.doi.org/10.1016/j.cels.2015.08.014

SUMMARY

In cancer genomics, recurrence of mutations in independent tumor samples is a strong indicator of functional impact. However, rare functional mutations can escape detection by recurrence analysis owing to lack of statistical power. We enhance statistical power by extending the notion of recurrence of mutations from single genes to gene families that share homologous protein domains. Domain mutation analysis also sharpens the functional interpretation of the impact of mutations, as domains more succinctly embody function than entire genes. By mapping mutations in 22 different tumor types to equivalent positions in multiple sequence alignments of domains, we confirm well-known functional mutation hotspots, identify uncharacterized rare variants in one gene that are equivalent to well-characterized mutations in another gene, detect previously unknown mutation hotspots, and provide hypotheses about molecular mechanisms and downstream effects of domain mutations. With the rapid expansion of cancer genomics projects, protein domain hotspot analysis will likely provide many more leads linking mutations in proteins to the cancer phenotype.

INTRODUCTION

The landscape of somatic mutations in cancer is extraordinarily complex, making it difficult to distinguish oncogenic alterations from passenger mutations. Many approaches use the recurrence of alterations in a single gene across tumor samples to identify potential driver genes. However, the molecular functions of genes are often pleiotropic, and in many cases it may not be a gene as an entity itself but rather the specific function of a gene or a set of genes that is under selective pressure in cancer. For example, in T cell acute lymphoblastic leukemia, the transmembrane signaling receptor *NOTCH1* is activated by mutations in the heterodimerization and the PEST domains (rich in proline [P], glutamic acid [E], serine [S], and threonine [T]; Weng et al., 2004), while in squamous cell carcinomas, notch signaling has a tumor-suppressive role and notch receptors (*NOTCH1–NOTCH4*) are inactivated by mutations in the ligand binding epidermal growth factor (EGF)-like domains (Wang et al., 2011). Thus, an alternative approach to assessing the relevance of somatic alterations is to determine the recurrence of mutations in genes involved in similar molecular functions. One powerful method for systematically assessing common biological function of genes is through the analysis of protein domains, which are evolutionarily conserved, structurally related functional units encoded in the protein sequence of genes (Holm and Sander, 1996; Chothia et al., 2003). By coupling the observation of mutations across genes in a domain family together, it may be possible to identify additional functional alterations that confer a selective, functional advantage to cancer cells and learn more about the details of pathway organization downstream of activated domains.

Large cross-institutional projects, such as the Cancer Genome Atlas (TCGA), have recently profiled the major human cancer types genomically, including glioblastoma (McLendon et al., 2008), lung (Hammerman et al., 2012; Ding et al., 2008), ovarian (Bell et al., 2011), breast (Koboldt et al., 2012), endometrial (Kandoth et al., 2013), kidney (Creighton et al., 2013), and colorectal cancer (Cancer Genome Atlas Network, 2012). Through whole-exome sequencing of tumor-normal pairs, these and other studies have provided catalogs of somatically mutated genes that are frequently altered and therefore likely associated with disease development. However, despite a collection of mutation data from nearly 5,000 samples encompassing 21 tumor types, the results from a recent pan-cancer study illustrate that by using recurrence of mutations in genes, thousands of samples per tumor type are needed to confidently identify genes that are mutated at low but clinically relevant frequencies (2%–5%) (Lawrence et al., 2014).

Several analytical approaches have been developed to detect genes associated with oncogenesis (Gonzalez-Perez and Lopez-Bigas, 2012; Dees et al., 2012; Lawrence et al., 2014). One of these widely applied algorithms, MutSigCV, compares the gene-specific mutation burden to a background model using silent mutations in the gene and gene neighborhood as well as contextual information (DNA replication timing and general level of transcriptional activity) to estimate the probability that the gene is significantly mutated (Lohr et al., 2012; Lawrence et al., 2014). Additional approaches have been developed to predict the functional impact of specific amino acid changes. These approaches generally rely on analyzing physico-chemical properties of amino acid substitutions (e.g., changes in size and polarity), structural information (e.g., hydrophobic propensity and surface accessibility), and the evolutionary conservation of the

mutated residues across a set of related genes (Reva et al., 2011; Yue et al., 2006; Bromberg et al., 2008; Ng and Henikoff, 2003; Adzhubei et al., 2010). Other approaches analyze mutations across sets of functionally related genes to test for a possible enrichment of mutation events in signaling pathways (Cerami et al., 2010; Ciriello et al., 2012; Hofree et al., 2013; Torkamani and Schork, 2009) or investigate how alterations/modifications alter protein-protein or protein-nucleic interactions (Betts et al., 2015) as well as phosphorylation-dependent signaling motifs (Reimand and Bader, 2013; Reimand et al., 2013).

Protein domains represent particular sequence variants that have been formed over evolution by duplication, recombination, or both (Holm and Sander, 1996; Chothia et al., 2003). Domains often encode structural units associated with specific cellular tasks, and large proteins with multiple domains can have several molecular functions each exerted by a specific domain. The structure-function relationship encoded in domains has been used as a tool for understanding the effect of mutations across functionally related genes. For example, some of the most frequent oncogenic mutations in human cancer affect analogous residues of the activation segment of the kinase domain and cause constitutive activation of several oncogenes, including *FLT3* D835 mutations in acute myeloid leukemia, *KIT* D816 mutations in gastrointestinal stromal tumors, and *BRAF* V600 mutations in melanoma (Dibb et al., 2004; Greenman et al., 2007). Proteome-wide bioinformatics analysis of mutations in domains has been performed to identify domains enriched for alterations (Nehrt et al., 2012; Peterson et al., 2012; Yang et al., 2015) as well as to detect significantly mutated domain hotspots using multiple sequence analysis (Peterson et al., 2010; Yue et al., 2010). We here extend upon these analyses by performing a systematic pan-cancer analysis of recurrence of mutations in protein domains (hotspots and enrichment of mutations across the domain body) and identify dozens of unreported cancer-associated mutations that are not detected using standard gene-based approaches.

Here, we performed a systematic and comprehensive analysis of mutations in protein domains using data from more than 5,000 tumor-normal pairs from 22 cancer types profiled by the TCGA consortium and domains from the protein family database Pfam-A (Punta et al., 2012). Using multiple sequence analysis, we determined whether conserved residues in protein domains were affected by mutations across related genes and identified many putative ''domain hotspots.'' We further exposed rare mutations that associated with well-characterized oncogenic mutations, including the furin-like domain where uncharacterized mutations in *ERBB4* (S303F) are analogous to known oncogenic mutations in the same domain of *ERRB2* (S310F), suggesting similar functional consequences. In several cases, we associated rare mutations in potential cancer genes with therapeutically actionable hotspots in known oncogenes, underlining the potential clinical implications of our findings.

RESULTS

Mapping Somatic Mutations to Protein Domains

To systematically analyze somatic mutations in the context of conserved protein domains, we retrieved whole-exome sequencing data from 5,496 tumor-normal pairs of 22 different tumor types profiled by the TCGA consortium. To obtain a uniform dataset of mutation calls, annotation of somatic mutations were based on the publicly available data (October 2014) from the cBioPortal for cancer genomics data (Figure 1) (Cerami et al., 2012; Gao et al., 2013). After filtering out ultra-mutated samples and mutations in genes with low mRNA expression levels (Supplemental Experimental Procedures), the data consisted of a total of 727,567 mutations in coding regions with 463,842 missense, 192,518 silent, and 71,207 truncating or small in-frame mutations. Focusing on missense mutations, we observed that the relative proportion of amino acids affected by mutations varied considerably between cancer types (Figure S1A). These amino acid mutation biases are due to a combination of variations in the codon usage between different amino acids and the variations in the base-pair transitions and transversions observed between different cancer types (Lawrence et al., 2013; Alexandrov et al., 2013). Because of the high mutation rate of CG dinucleotides (cytosine nucleotide occurs next to guanine nucleotide) across all cancers, arginine (R) is the most frequently altered amino acid despite being the ninth most common amino acid as CG dinucleotides are present in four out of six of arginine's codons (Figure S1B).

We next mapped the mutations to conserved protein domains obtained from the database of protein domain families, Pfam-A version 26.0 (Punta et al., 2012) (Figure 1A). Overall, 4,401 of 4,758 unique Pfam domains in the human genome were mutated at least once across all samples. The fraction of missense mutations that map to domains (46.7%, or 216,676 of 463,842) was consistent across samples and tumor types and was similar to the proportion of the proteome assigned as conserved domains (45.4%; Figure S1A).

Identification of Domains with Enriched Mutation Burden

Our first aim was to identify domains that have an increased mutation burden. We defined the domain mutation burden as the total number of missense mutations in a domain, excluding domains only present in only one gene. After tallying mutations across samples, the domain with the highest mutation burden was the protein kinase domain with 7,203 mutations in 353 genes (not including genes with tyrosine kinase domains), while the P53 domain present in *TP53*, *TP63*, and *TP73* had the most mutations when normalizing for the domain length and the size of the domain family. To systematically investigate whether the mutation burden for a given domain was larger than would be expected by chance, we performed a permutation test that takes into account the number of mutations within and outside of the domain, the domain length, and the length and number of genes in the domain family. To specifically compare domain versus non-domain areas, we excluded other domains present in the domain-containing gene family. Assuming that each mutation is an independent event and that all residues of the protein have an equal chance of being mutated, we randomly reassigned all mutations 10^6 times across each gene separately and calculated whether the observed domain mutation burden was significantly different from the distribution of burdens observed by chance (Figure 1B).

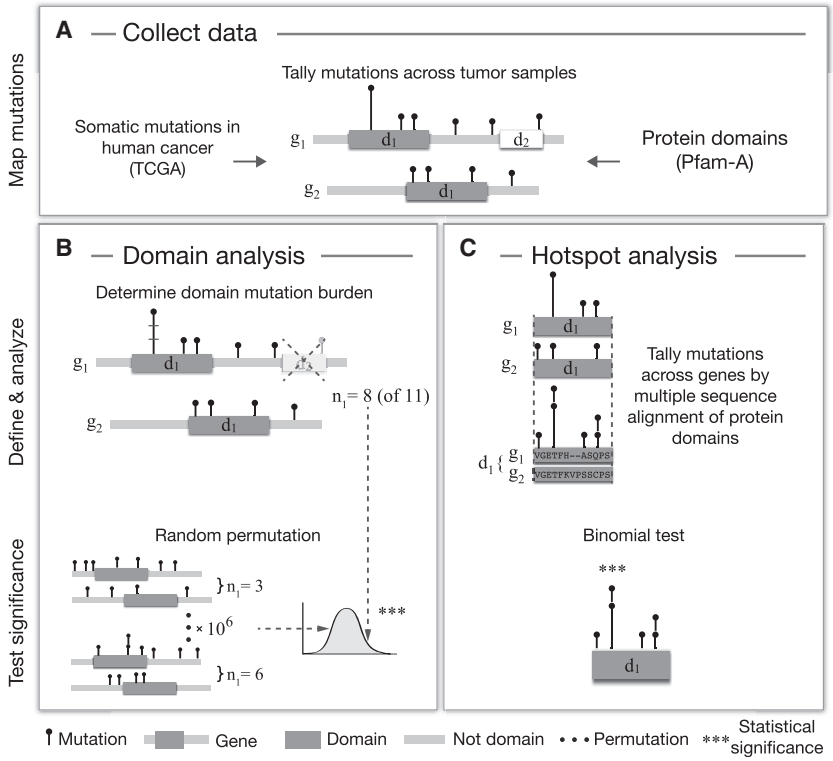

Figure 1. Workflow for Analyzing Recurrently Mutated Protein Domains in Cancer

(A–C) Missense mutation data from recent genomic profiling projects of human cancers (TCGA) are collected, and all mutations are tallied across tumor samples and cancer types (A). Mutations are mapped to protein domains obtained from the Pfam-A database, which contains a manually curated set of highly conserved domain families in the human proteome. Two separate analyses are performed on these data to (B) identify domains enriched for missense mutations and (C) detect mutation hotspots in domains through multiple sequence alignment. In the first analysis (B), the observed mutation burden (n_1) of a specific domain (d_1) is calculated by counting the total number of mutations in all domain-containing genes (g_1&g_2). Mutations in other domains (e.g., d_2) are excluded. A permutation test is applied to determine whether the observed mutation burden (n_1 = 8) is larger than expected by chance. Mutations are randomly shuffled 10^6 times across each gene separately, and the observed mutation count is compared to the distribution of randomly estimated mutation counts. In the second analysis (C), domains are aligned across related genes by multiple sequence alignment and mutations are tallied at each residue of the alignment. A binomial test is applied to determine whether the number of mutations at a specific residue is significantly different from the number of mutations observed at other residues of the alignment.

Using this permutation approach, we identified 14 domains that were significantly enriched for missense mutations within the domain boundaries compared to other areas of the same genes ($p < 0.05$, Bonferroni corrected; Figure 2; Table 1). As both the number of gene members per domain (domain family) and the number of mutations per gene vary greatly, we wanted to distinguish between two cases: (1) only a single or a few genes in the domain family contributed to the domain mutation burden, and (2) genes contributed more evenly to the mutations in the domain. We were particularly interested in the latter because mutations in domains contributed by many infrequently mutated genes may represent new functional alterations that would not have been discovered using traditional gene-by-gene approaches. To investigate this, we calculated an entropy score ($\overline{S}$) that was normalized to the size of the domain family, so a low score indicates that the mutation burden is unevenly distributed between domain-containing genes, and a high score indicates that the mutation burden is distributed evenly among the genes in the domain family (Supplemental Experimental Procedures).

As expected, we found that the von Hippel-Lindau (VHL) and the P53 domains were significantly enriched for mutations and had low entropy scores because they were dominated by mutations in the canonical tumor suppressor genes *VHL* and *TP53*, respectively (Figure 2; Table 1, rows 6 and 9). On the other end of the spectrum, the KAT11 domain encoding the lysine acetyltransferase (KAT) activity of *CREBBP* and *EP300* was significantly mutated and had a high normalized entropy score with around 30 mutations in each gene (Table 1, row 1). *CREBBP* and *EP300* are transcriptional co-activators that regulate gene expression through acetylation of lysine residues of histones and other transcription factors (Liu et al., 2008). In our analysis, head and neck squamous cell carcinoma (HNSC) was the tumor type with most mutations in KAT11, and nearly half fell in the domain (14 of 29) that spans only about 4% of the length of both *CREBBP* and *EP300* (Figure S2). One of the two genes (*EP300*) has previously been reported as significantly altered in HNSC (Lawrence et al., 2014). Supporting the enrichment of mutations in the KAT11 domain, inactivating mutations in KAT11 have been associated with oncogenesis in tumor types not part of this analysis, including B cell lymphoma (Pasqualucci et al., 2011; Cerchietti et al., 2010; Morin et al., 2011) and small-cell lung cancer (Peifer et al., 2012). In small-cell lung cancer, *CREBBP* and *EP300* were reported to be deleted in a mutually exclusive fashion (Peifer et al., 2012), which often indicates that genes are functionally linked (Ciriello et al., 2012).

Confirming canonical mutation events in cancer, we found mutations clustering in domains of genes involved in receptor tyrosine kinases (RTKs) signaling, including the tyrosine kinase domain itself (Pkinase_Tyr), the furin-like domain involved in RTK aggregation, and downstream signaling through genes with the ras GTPase domain and the phosphatidylinositol 3-kinase (PI3Ka) domain (Table 1, rows 2, 3, 4, and 12). These domains have also been reported in other systematic studies of mutations in domains (Yue et al., 2010; Nehrt et al., 2012), consistent with the fact that the RTK signaling pathways are often hijacked in cancer (Hanahan and Weinberg, 2011). In a similar manner, we identified multiple domains in genes that have previously been associated with cancer, including the DNA-binding forkhead domain in Fox family transcription factors and the frizzled domain in G-protein-coupled receptors of the Wnt signaling pathway. Interestingly, these domains have high

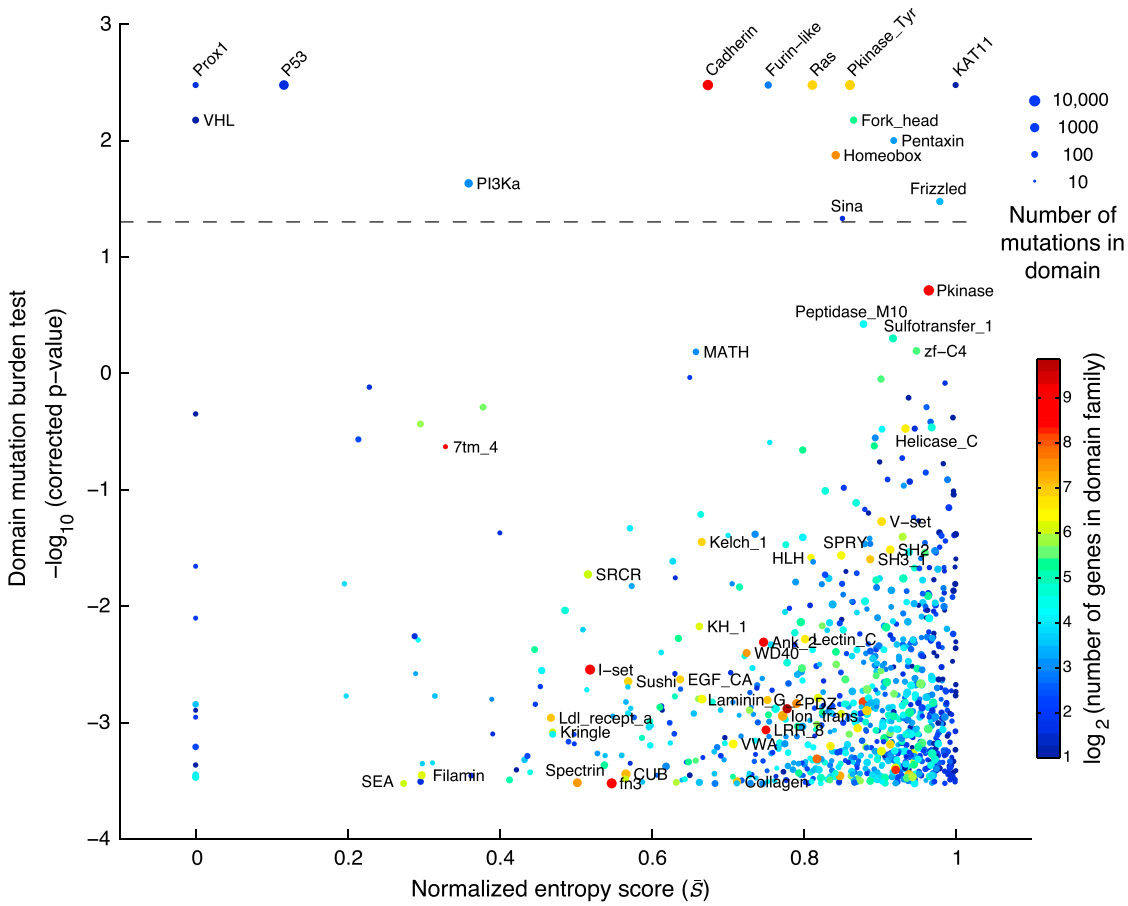

Figure 2. Identification of Protein Domains Enriched for Missense Mutations

The estimated significance level of the domain mutation burden test is plotted against the domain entropy score ($\bar{S}$). The domain mutation burden test captures the enrichment of mutations within the domain boundaries compared to non-domain areas of the same genes. The entropy score captures the degree to which individual or multiple genes contribute to the mutations in the domain, where low and high scores indicate that the mutation burden is unevenly or evenly distributed between domain-containing genes, respectively. $\bar{S}$ is normalized to the highest possible score so that, when $\bar{S} = 1$, all genes are evenly mutated, and when $\bar{S} = 0$, then only one gene is mutated. Domains with a significant mutation burden are indicated above the dashed line ($p < 0.05$, Bonferroni corrected). The sizes of the dots reflect the number of mutations in each domain. Domains are color coded by the number of genes in the domain family.

entropy scores with a substantial amount of mutations contributed by genes not reported as altered in a recent pan-cancer study (see the italics and underlined formatting in Table 1, rows 8 and 13) (Lawrence et al., 2014). Thus, from the perspective of the structure-function relationship encoded in domains, these are candidate cancer driver genes due to the enrichment of mutations in these functional regions.

We also identified several domain families in which most of the genes had no apparent link to cancer. Such domains include the homeobox domain involved in DNA binding and the cadherin domain involved in cell adhesion (Table 1, rows 5 and 11). As cell-cell adhesion and DNA binding are critical cellular processes, it is plausible that domain-contained genes involved in these processes are under positive selective pressure in the cancer environment, although it remains to be tested whether mutations in these domains are functionally disruptive and may play a critical role in cancer. Several additional domains were found to be enriched for mutations and may potentially be of interest in a cancer context (Table 1).

Protein Domain Alignment Reveals Mutation Hotspots across Related Genes

We next aligned each domain using multiple sequence alignment and tallied mutations across analogous residues of domain-containing genes (Figure 1C). The goals of this analysis were to identify new domain hotspots with recurrent mutations across functionally related genes and to associate hotspots in well-established cancer genes with rare events in genes not previously linked to cancer. We used a binomial test to determine whether a mutation peak at a specific residue was significantly different from other residues in the domain alignment, and we applied the same entropy analysis to investigate the degree to which individual or multiple genes contributed mutations to each hotspot. Based on Bonferroni-corrected p value ($p < 0.05$), we identified 82 significant hotspots in 42 different domains (Table S1) with the subset of hotspots detected in mutations in at least two genes presented in Table 2.

To assess the power of the domain-based approach to identify mutations that would have been missed using a traditional

Table 1. Protein Domains Significantly Enriched for Mutations

Row	Domain	Genes (#)	p-val ($-\log_{10}$)	$\bar{S}$	Mutations (#)	e_d	Top Genes (gene symbol and # of mutations)	Top Cancers (cancer and # of mutations)
1	KAT11	2	2.48	1	65	1.94	*CREBBP* 33; *EP300* 32	HNSC 14; BLCA 10
2	Pkinase_Tyr	120	2.48	0.861	2059	1.17	*BRAF* 427; *EGFR* 50; *ERBB2* 43	SKCM 428; THCA 246
3	Ras	124	2.48	0.811	1369	1.08	*KRAS* 269; *NRAS* 177; *HRAS* 46	SKCM 206; COADREAD 166
4	Furin-like	7	2.48	0.753	147	1.77	*EGFR* 67; *ERBB3* 30; *ERBB2* 23	GBM 42; LGG 14
5	Cadherin	614	2.48	0.674	3358	1.06	FAT4 214; FAT3 184; *FAT1* 116	SKCM 607; LUAD 474
6	P53	3	2.48	0.116	1333	1.63	*TP53* 1301; TP63 23; TP73 9	OV 182; BRCA 171
7	Prox1	3	2.48	0	56	1.05	PROX1 56; PROX2 0	HNSC 13; SKCM 11
8	Fork_head	42	2.18	0.866	165	1.4	*FOXA1* 25; FOXA2 10; FOXK2 10	BRCA 22; SKCM 18
9	VHL	2	2.18	0	103	1.24	*VHL* 103; VHLL 0	KIRC 95; SKCM 2
10	Pentaxin	9	2	0.918	99	1.42	NPTX2 22; SVEP1 17; NPTXR 16	SKCM 23; HNSC 13
11	Homeobox	190	1.87	0.842	375	1.23	ZFHX4 28; NKX3-1 11; ONECUT2 11	SKCM 48; UCEC 44
12	PI3Ka	8	1.63	0.359	356	1.21	*PIK3CA* 296; PIK3CG 20; PIK3CB 13	BRCA 126; UCEC 44
13	Frizzled	11	1.48	0.979	164	1.21	FZD10 24; FZD9 20; FZD3 19	BRCA 18; LUAD 18
14	Sina	3	1.33	0.851	31	1.43	SIAH2 16; SIAH1 12; SIAH3 3	UCEC 5; COADREAD 4

Domains are listed by their Pfam domain identifiers, the number of genes in the domain family, the Bonferroni-corrected p value, the entropy score ($\bar{S}$), the number of mutations in the domain, the mutation enrichment score (e_d) expressed as the ratio of the observed number of domain mutations to the expected number of domain mutations, the genes with the most domain mutations, and the two cancers with most domain mutations. Genes are in italics if they were reported to be significantly mutated in a recent pan-cancer study (Lawrence et al., 2014) and underlined if not. The list is sorted by p value followed by entropy score.

gene-by-gene approach, we systematically compared the two approaches using the same dataset and similar binomial statistics. Using the domain-based approach, we identifying an additional 68 mutations in genes that were not detected when analyzing genes individually, indicating that the domain-based analysis complements the gene-based (Figure S3; Table S2). Although previous studies have used multiple sequence analysis to discover hotspots in domains (Peterson et al., 2010; Yue et al., 2010), these studies were conducted before the recent wave of published cancer genomics studies, hindering a direct performance comparison due to extensive differences of data availability at the time of analysis. A recent report investigated mutations in domains using current cancer genomics datasets (Yang et al., 2015); however, this analysis did not include multiple sequence alignment and hotspot detection across domain-containing genes, making a direct comparison of the methods infeasible.

We recapitulated several well-known hotspots in domains where only one gene was mutated such as the P53 and PI3Ka domains with mutations in *TP53* and *PIKC3A*, respectively (entropy approximately equal to 0; Figure 3; Table 2, rows 13, 14, and 17). We also confirmed several known domain-specific hotspots such as the isocitrate/isopropylmalate dehydrogenase domain (Iso_dh) with homologous mutations in *IDH1* (position R132) and *IDH2* (R172) as well as the ras domain with mutations in *KRAS*, *NRAS*, and *HRAS* at positions G12, G13, and Q61 in the GTP binding region (Table 2, rows 3, 7, 8, and 10). Furthermore, we found that well-characterized hotspots in *KIT* D816 in acute myeloid leukemia (AML), *FLT3* D835 in AML, and *BRAF* V600 in thyroid carcinoma and melanoma aligned perfectly in the conserved activation segment of the tyrosine kinase domain (Table 2, row 11). These mutations are known to cause constitutive kinase activity, which promotes cell proliferation independent of normal growth factor control (Hanahan and Weinberg, 2011; Dibb et al., 2004). We further superimposed the crystal structures of the three proteins and found that the residues overlap in structure space (Figure S4), offering support that the alignment approach captures structurally relevant information. Notably, in the same domain hotspot many singleton mutations in lung adenocarcinoma and lung squamous cell carcinoma mapped to the equivalent position in other RTKs, including *EPHA2* V763M, *FGFR1* D647N, *PDGFRA* D842H, and three mutations in *EGFR* L861Q. Although these are rare events in lung cancer, this analysis reveals that they likely affect the same activation loop residue and may be therapeutically actionable in a similar manner as the hotspot mutations in *KIT*, *FLT3*, and *BRAF*.

Similar to the previous analysis of entropy in recurrently mutated domains, we were interested in domain hotspots with high entropy scores. Again, the lysine acetylase domain, KAT11, was identified with high entropy for a significant hotspot at position 94 of the domain alignment with mutations in *EP300* at D1399 and *CREBBP* at D1435 (Table 2, row 1). These sites are located in the substrate binding loop of KAT11, and mutations in these residues affect the structural conformation of the substrate binding loop (Liu et al., 2008). Recently, both genes have been implicated in other cancers not analyzed here such as small-cell lung cancer (Peifer et al., 2012) and B cell lymphoma (Pasqualucci et al., 2011; Cerchietti et al., 2010; Morin et al., 2011). Confirming the functional relevance of the identified hotspot, both *EP300* D1399 and *CREBBP* D1435 mutations have been found to reduce lysine acetylase activity in vitro (Peifer et al., 2012; Pasqualucci et al., 2011; Liu et al., 2008). We additionally identified a potential hotspot in KAT11 at position 105 with mutations in *CREBBP* (R1446), although this hotspot was not significant when correcting for multiple hypothesis testing ($p = 2.6e^{-6}$, corrected $p = 0.59$; Figure 4A). *CREBBP* R1446 is

Table 2. Identified Mutation Hotspots in Protein Domains

Row	Domain	Genes (#)	Position	p Value ($-\log_{10}$)	$\overline{S}$	Mut (#)	Top Gene 1 (# mut, gene, site)	Top Gene 2 (# mut, gene, site)	Top Cancer (# mut, cancer)
1	KAT11	2	94	10	0.88	10	7 *EP300* D1399	3 *CREBBP* D1435	3 BLCA
2	Orn_DAP_Arg_deC	3	86	10	0.28	11	10 AZIN1 S367	1 ODC1 R369	10 LIHC
3	Ras	124	17	10	0.27	56	31 *KRAS* G13	11 *NRAS* G13	12 COADREAD
4	MH2	8	46	10	0.25	14	11 *SMAD4* R361	3 SMAD3 R268	8 COADREAD
5	Furin-like	7	119	10	0.20	30	27 *EGFR* A289	2 *ERBB3* G284	23 GBM
6	PI3K_C2	7	130	10	0.19	17	15 *PIK3CA* E453	2 PIK3CB E470	7 BRCA
7	Ras	124	88	10	0.18	189	142 *NRAS* Q61	22 *HRAS* Q61	78 SKCM
8	Iso_dh	5	128	10	0.14	292	274 *IDH1* R132	18 *IDH2* R172	232 LGG
9	WD40	170	16	10	0.13	37	31 *FBXW7* R465	2 *FBXW7* Y545	12 COADREAD
10	Ras	124	16	10	0.12	224	192 *KRAS* G12	17 *NRAS* G12	74 COADREAD
11	Pkinase_Tyr	120	291	10	0.09	415	382 *BRAF* V600	14 *FLT3* D835	235 THCA
12	Recep_L_domain	14	52	10	0.08	17	16 *ERBB3* V104	1 *ERBB2* I101	5 COADREAD
13	P53	3	181	10	0.07	141	139 *TP53* R273	2 TP63 R343	44 LGG
14	PI3Ka	8	27	10	0.02	164	163 *PIK3CA* E545	1 PIK3CB E552	66 BRCA
15	Furin-like	7	136	7.24	0.22	13	11 *ERBB2* S310	2 ERBB4 S303	4 STAD
16	zf-H2C2_2	940	7	7.21	0.62	79	2 ZNF208 R613	2 ZNF286A R430	27 UCEC
17	P53	3	157	5.25	0.14	29	28 *TP53* R249	1 TP63 R319	8 LIHC
18	RasGAP	12	23	4.03	0.53	8	3 RASAL1 R342	2 *NF1* R1276	2 HNSC
19	BicD	2	570	3.3	0.97	5	3 BICD2 R635	2 BICD1 R633	2 SKCM
20	Pro_isomerase	19	31	3.13	0.48	9	4 PPIAL4G R37	2 PPIG R41	7 SKCM
21	DUF3497	11	3	2.91	0.40	7	4 BAI3 R588	2 ELTD1 K132	4 SKCM
22	MT	15	36	2.79	0.14	8	7 DNAH5 D3236	1 DNAH11 H3139	8 SKCM
23	Choline_transpo	5	186	2.56	0.42	5	3 SLC44A1 R437	2 SLC44A4 R496	1 BRCA
24	bZIP_2	9	21	2.4	0.61	6	2 HLF R243	2 NFIL3 R91	2 UCEC
25	Fork_head	42	88	2.4	0.46	11	3 FOXP1 R514	2 FOXJ1 R170	4 COADREAD

The detected domain hotspots are listed by their Pfam domain identifiers, the number of genes in the domain family, the position of the hotspot in the domain alignment, the Bonferroni-corrected p values, the entropy score ($\overline{S}$), the number of mutations in the hotspot, the two genes with the most mutations in the hotspot, and the cancer type with most mutations in the hotspot. Genes are in italics if they were reported to be significantly mutated in a recent pan-cancer study (Lawrence et al., 2014) and underlined if not. The list is sorted by p value followed by entropy score. Hotspots in domains where only one gene was mutated ($\overline{S}$ = 0) were excluded. All significant domain hotspots (82) are provided in (Table S1).

also located within the substrate binding loop (Liu et al., 2008), and R1446 mutations have been found in B cell neoplasms (Pasqualucci et al., 2011).

Associating Rare Mutations with Known Oncogenic Hotspots

The MAD homology 2 (MH2) domain is found in *SMAD* genes and mediates interaction between SMAD proteins and their interaction partners through recognition of phosphorylated serine residues (Wu et al., 2001). We found the known R361H/C hotspot mutation in *SMAD4* (Shi et al., 1997; Ohtaki et al., 2001) aligned with three R268H/C mutations in *SMAD3* (Figure 4B; Table 2, row 4). In both proteins these residues are located in the conserved loop/helix region that is directly involved in binding *TGFBR1* (Shi et al., 1997). R361C mutations inactivate the tumor suppressor *SMAD4* (Shi et al., 1997), and recently, R268C mutations in *SMAD3* were also found to repress SMAD3-mediated signaling (Fleming et al., 2013), supporting our association of rare arginine mutations in *SMAD3* with known inactivating mutations in *SMAD4*. The majority of the mutations in the hotspot were from colorectal adenocarcinoma samples (COADREAD), and it is known that *SMAD* genes are recurrently mutated in this disease (Fleming et al., 2013). Interestingly, we found a non-significant (p = 0.25) tendency toward better survival for patients with hotspot mutations in colorectal cancer, although more data are needed to confirm this, to our knowledge, unreported observation (Figure S5).

We associated several known hotspots in well-characterized cancer genes with rare but potentially functional mutations in genes not frequently mutated in cancer. For example, we found rare mutations in *PIK3CB* at E470 and at E552 in the PI3K_C2 domain and PI3Ka domain, respectively, that associated with known recurrent hotspots in *PIK3CA* (Table 2, rows 6 and 14). Furthermore, in the cysteine-rich Furin-like domain, which is involved in receptor aggregation and signaling activation of ERBB-family RTKs, we identified several significant hotspots, including rare mutations in *ERBB3* (G284R) and *ERBB2* (A293V) that aligned with the known activating driver mutations in *EGFR* (A289V/T) in glioblastoma (Figure 4C) (Lee et al., 2006). Recently, one of these mutations, *ERBB3* G284R, was found to promote tumorigenesis in mice (Jaiswal et al., 2013), suggesting that the singleton *ERBB2* A293V mutation found in

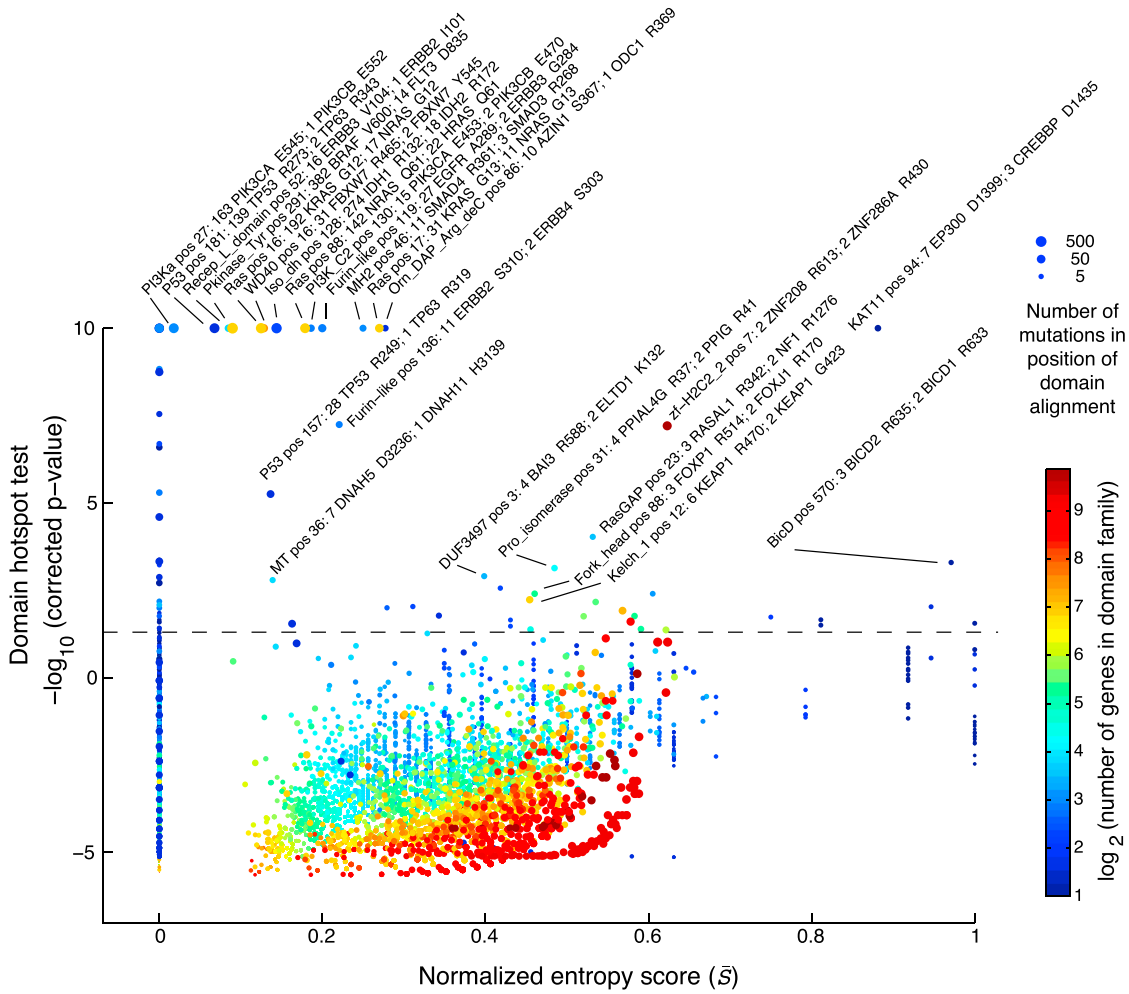

Figure 3. Domain Alignment Detects Mutation Hotspots across Related Genes

The estimated significance level of each mutation hotspot in the domain alignment is plotted against the domain entropy score ($\bar{S}$), which is described elsewhere. Significant hotspots are indicated above the dashed line ($p < 0.05$, Bonferroni corrected). The maximal significance was set to 10 ($-\log_{10}$ [p value]). Hotspots are named by the Pfam identifiers followed by the position in the domain alignment and the number of mutations in the top two mutated genes. The size of the dots reflects the number of mutations at each residue, and the dots are color coded by the number of domain-containing genes in the genome.

a melanoma sample could represent an infrequent oncogenic event. We also identified a hotspot at position 137 of the alignment with rare S303F mutations in *ERBB4* aligning with S310F/Y mutations in *ERBB2*. Interestingly, in a functional analysis of *ERBB2* mutations in lung cancer cell lines, S310F/Y mutations were found to increase *ERBB2* signaling activity, promote tumorigenesis, and enhance sensitivity to *ERBB2* inhibitors in vitro (Greulich et al., 2012). Future work will show whether analogous mutations in *ERBB4* (S303F) may have similar effects.

Identification of New Hotspots in Protein Domains

We also identified several additional hotspots in domains with mutations in genes not previously associated with cancer. We detected a hotspot in the peptidyl-prolyl isomerase domain (Pro_isomerase) with nine mutations distributed among *PPIAL4G* (R37C), *PPIG* (R41C), *PPIA* (R37C), *PPIE* (R173C), and *PPIL2* (I308F) (Figure 5A). The Pro_isomerase domain, which is distinct from the rotamase domain of *PIN1*, is present in genes that catalyze *cis-trans* isomerization of proline imidic peptide bonds and have been implicated in folding, transport, and assembly of proteins (Göthel and Marahiel, 1999). Seven of the nine mutations found in this hotspot were from melanoma samples, and interestingly, we found that in melanoma these mutations correlate with significant upregulation of about a dozen genes, including the cancer-testis antigens *CTAG2*, *CTAG1B*, *CSAG2*, and *CSAG3* (Figure S6).

The forkhead domain mediates DNA binding of forkhead box (Fox) transcription factors and encodes a conserved "winged helix" structure comprising three α helices and three β sheets flanked by one or two "wing"-like loops (Carlsson and Mahlapuu, 2002). In the forkhead domain, we identified a hotspot with 11 mutations distributed among *FOXP1* (R514C/H), *FOXK2* (R307C/H), *FOXK1* (R354W), *FOXJ1* (R170G/L), and *FOXP4* (R516C) in several different cancer types (Figure 5B). The identified hotspot was located in the third α helix (H3), which exhibits a high degree of sequence homology across Fox proteins and

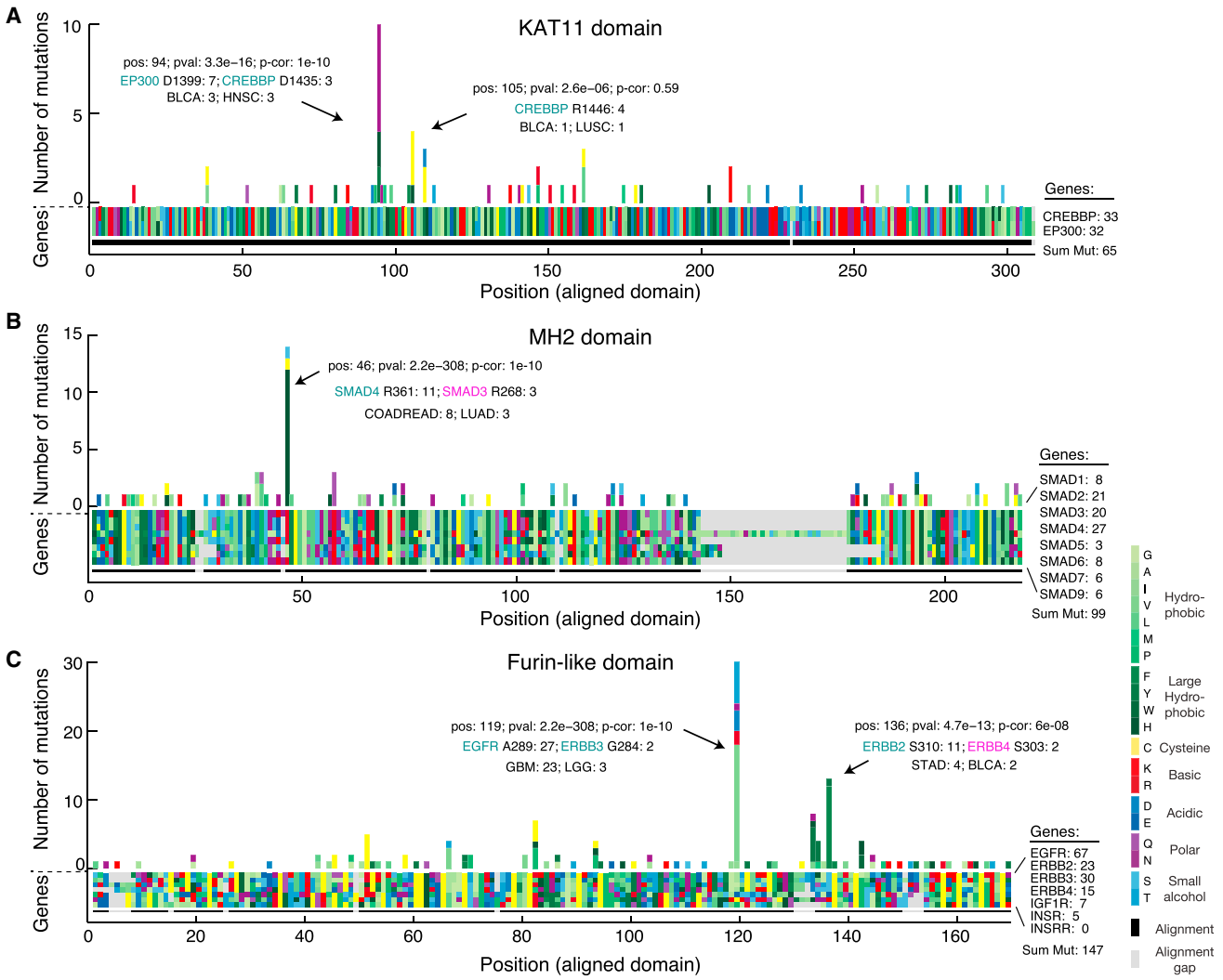

Figure 4. Multiple Sequence Alignment of Domains Identifies Mutation Hotspots and Associates Rare Mutations with Known Oncogenic Hotspots

(A) The amino acid sequence alignment of the KAT11 histone acetylate domain in *CREBBP* (positions 1342–1648) and *EP300* (positions 1306–1612) is represented as a block of two by 308 rectangles. Using the resulting alignment coordinates, missense mutations are tallied across the domains of the two genes. Both amino acids of the alignment (block) and the resulting amino acids due to mutations (histogram) are color coded by their biochemical properties. Alignment gaps are indicated by gray rectangles. Significant hotspots are indicated with position in alignment (pos), p value (pval), Bonferroni-corrected p value (p-cor), and number of mutations in top mutated genes and cancer types.

(B and C) Similar plots are shown for the MAD homology 2 (MH2) domain involved in SMAD protein-protein interactions (B) and the furin-like domain involved in RTK aggregation and signal activation (C).

binds to the major groove of DNA targets. Specifically, the arginine residue that we found mutated forms direct hydrogen bonding with DNA in both *FOXP* and *FOXK* family transcription factors (Figures 5C and 5D) (Wu et al., 2006; Stroud et al., 2006; Chu et al., 2011; Tsai et al., 2006). Furthermore, experimental R307A substitution in *FOXK2* abolishes DNA binding (Tsai et al., 2006), suggesting that the identified arginine mutations may play an important role in cancer by inhibiting DNA binding of *FOXP*, *FOXK*, and related Fox transcription factors, although the hypothesis that the identified forkhead domain hotspot is an inactivating mutational event remains speculative.

We identified several other domain hotspots of potential interest such as a hotspot in the rasGAP GTPase activating domain with mutations in the tumor suppressors *NF1*, *RASA1*, and *RASAL1*; a hotspot in the kelch motif (Kelch 1 domain) with mutations in *KEAP1* and *KLHL4*; as well as a hotspot in a domain of unknown function, DUF3497 (Figure S7). The potential biological consequence of these mutations remains to be elucidated. Many additional domain hotspots were identified, and we make all analysis of hotspots in protein domains available via an interactive web service at http://www.mutationaligner.org.

DISCUSSION

We have extended the principle of recurrence analysis for protein mutations observed in surgical cancer specimens. Instead of

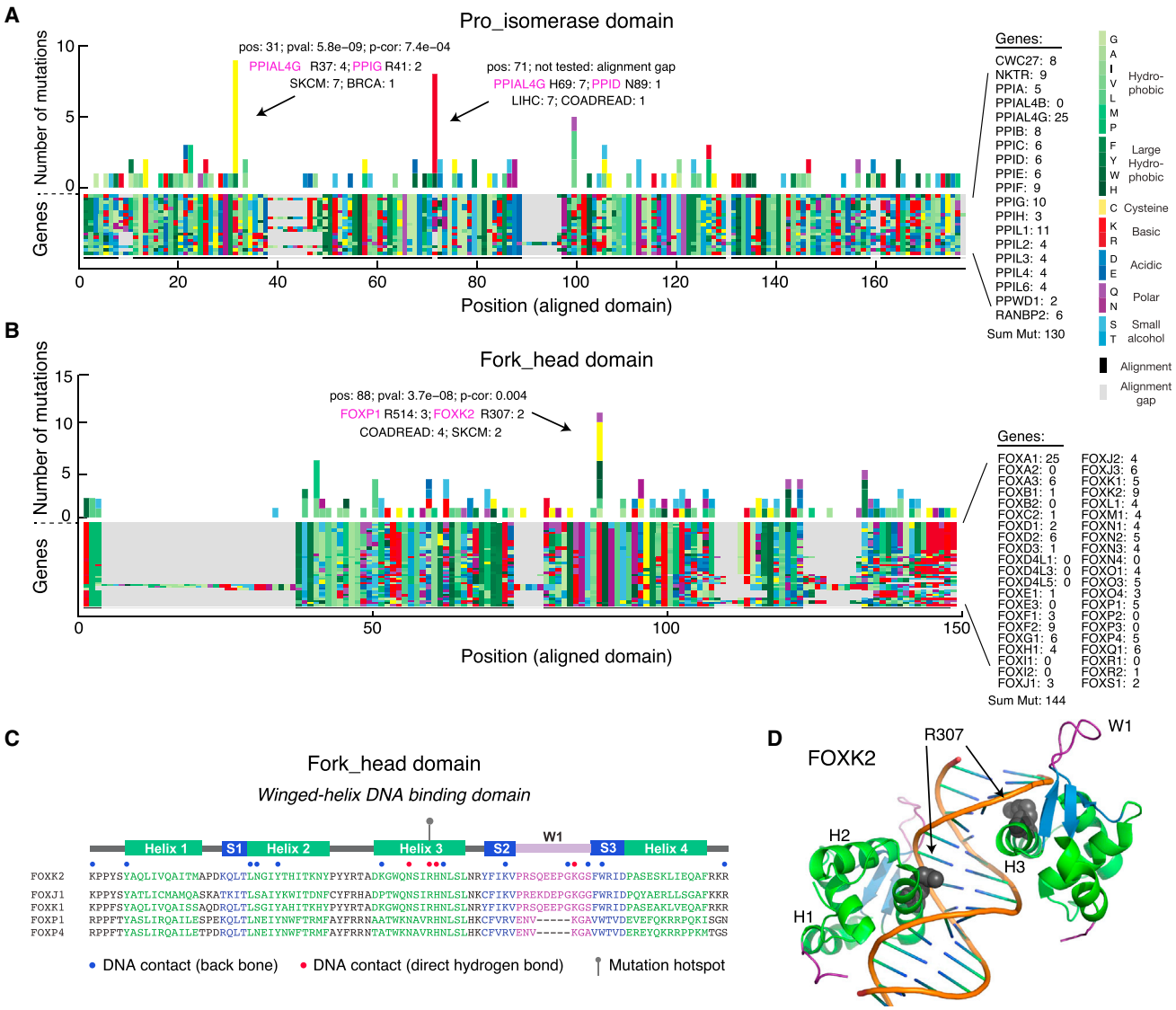

Figure 5. Identification of New Hotspots Affecting Conserved Residues of Protein Domains

(A and B) Missense mutations are tallied across multiple sequence alignments of genes containing the peptidyl-prolyl isomerase (Pro_isomerase) domain (A) and the forkhead domain (B).

(C) Secondary structure of the forkhead domain consisting of four α helices (H1–H4), three β sheets (S1–S3), and one wing-like loop (W1). Sequences are shown for selected Fox transcription factors that had mutations in the identified hotspot in H3. Of note, the selected genes have a fourth α helix rather than the canonical second wing-like loop found in other Fox genes.

(D) Ribbon drawing of the crystal structure of two *FOXK2* forkhead domains binding to a 16-bp DNA duplex containing a promoter sequence (PDB: 2C6Y) (Tsai et al., 2006). The R307 residue that we identified as mutated is shown with spheres.

only summing the occurrence of mutations over all tumor samples, we also sum over all homologous sisters of a protein domain. This increases the power of inferring likely functional mutations in several ways by enabling or providing: (1) higher statistical power to detect mutation hotspots (Figure S3; Table S2); (2) functional characterization of rare mutations that are in homologous positions relative to mutations with known functions (Figure 4; Table 2); (3) mechanistic clues or pathway linkage about the downstream effects of oncogenic mutations (Figure 4); (4) prediction of new therapeutically actionable alterations by homologous relationship to known drug targets (Figures 4C and S4); (5) identification of subpathways from selective alteration in a subset of upstream domains (Figure 4B); and (6) identification of novel domains with plausible oncogenic function based on aggregation of sub-threshold mutation counts (Figures 5 and S7). The impact of these methodological improvements on linking genotype and phenotype in cancer, as well as technical limitations, will be discussed below.

By extending the notion of recurrence of mutations from single genes to gene families, one immediately gains statistical power for interpreting recurrence (above random) of mutations across many cancer samples as evidence for a functional contribution

to oncogenesis or tumor maintenance. This is especially useful for mutations, which are infrequently observed in a particular domain in the family, but for which there are analogous alterations in sister domains in the domain family. For example, we identified a hotspot in the forkhead domain, where the crucial DNA-contacting arginine residue in the third helix of the forkhead-encoded winged-helix structure was mutated in several *FOXP* and *FOXK* family transcription factors. We speculate that this mutation in the DNA-binding part of the forkhead domain is a novel inactivating oncogenic event. This example illustrates the power of connecting the observation of mutations across common members of a domain family, enabling us to identify entirely new hotspots in domains with mutations in genes not previously associated with cancer.

Beyond the assertion of likely functional impact in cancer based on aggregate occurrence, we assigned specific functional consequences to some of the infrequent mutations in cases where the analogous residues in other family members have well-characterized functional roles. Because many protein domains have been functionally characterized, one of the strengths of our approach is that such knowledge can provide mechanistic insight into the potential effect of alterations. For example, we associated mutations in infrequently altered genes with mutations in paralogous genes that have previously been implicated in cancer (see, e.g., the identified hotspots in MH2, Furin-like, and PI3K_C2 domains). Thus, transfer of knowledge from well-studied oncogenes to less-studied homologs (''guilt by association'') can lead to testable hypotheses about the effect of rare alterations and hereby facilitate the functional interpretation of mutations in large cancer genomics datasets.

This analysis may also shed light on how oncogenic alterations in homologous domains are related in signaling pathways. While the effect of an oncogenic mutation on the function of an individual protein, such as signaling-independent enzymatic activity, may be known or can be ascertained experimentally, the downstream consequences are enmeshed in the full complexity of cell biological signaling pathways. Fortunately, the evolutionary relationships within a domain family plus the recurrence of specific residue alterations in the oncogenic selection process may provide clues as to similarity of mechanism and similarity of downstream consequences on cell physiology. For example, a furin-like domain is present in the extracellular region of both the ERBB2 and ERBB4 receptor tyrosine kinases. Our analysis clearly relates the known and fairly frequent oncogenic S310F/Y in *ERRB2* mutations with two uncharacterized mutations S303F in *ERBB4*. Both sets of mutations plausibly execute similar biophysical mechanisms, in which the replacement of a small amino acid with an O-H side chain (S) with a large hydrophobic amino acid (F or Y) in a conserved region modifies receptor multimerization and activates downstream mitogenic signaling (Greulich et al., 2012). This example, and others in the current dataset, is suggestive of the general principle that recurrent mutations in analogous positions in evolutionarily related protein domains share aspects of molecular mechanism as well as downstream cell biological effects.

That mutations in domains of related genes may have similar mechanistic consequence or effects on downstream signaling may also have therapeutic implications. In some cases plausibly actionable alterations can be identified through a homologous relationship to alterations in known drug targets. As the S310F/Y mutations in *ERBB2* sensitize cancer cell lines to the RTK inhibitors neratinib, afatinib, and lapatinib (Greulich et al., 2012), the same may be true for the analogous S310F/Y mutations in *ERBB4*. Furthermore, using sequence and 3D structure analysis of the tyrosine kinase domain, we also find that the canonical hotspots of *BRAF* (V600E), *FLT3* D835Y, and *KIT* D816V superimpose in the activation loop of the kinase domain controlling the enzymatic activity state (Figure S4). Notably, we found four *EGFR* L861Q/R mutations in lung cancer affecting an analogous residue in the activation loop. Based on the conserved structure-function relationship of the tyrosine kinase domain, these rare *EGFR* L861Q/R mutations may also represent activating events and could therefore be therapeutically actionable in analogy to the targetable *BRAF* V600E mutations. Encouragingly, non-small-cell lung cancer patients with *EGFR* L861 mutations have recently shown positive clinical response when treated with *EGFR*-targeted therapy (Wu et al., 2011). In the spirit of personalized therapy and basket clinical trials (Garraway and Lander, 2013), this type of convergence of downstream consequences of analogous mutations may suggest specific therapeutic choices for an additional set of observed cancer-associated mutations.

The mutational patterns across a set of sequence-similar domains may also be useful in elucidating fine-grained detail of pathway signaling, such as a useful distinction between subpathways. For example, in the current dataset, out of the eight members of the MH2 domain-containing SMAD family, only *SMAD3* and *SMAD4* are mutated at analogous positions involved in *TGFBR1* binding. Although there is inherent uncertainty in any finite dataset, this observation raises the hypothesis that signaling events of *SMAD3* and *SMAD4* in cancer—or perhaps in general—are more closely related than those involving other MH2 domain-containing proteins. In general, on the basis of mutational patterns in a large gene family, one may be able to uncover functional similarity between members of a family and thereby predict which subset of genes are involved in similar processes or particular signaling subpathways.

These examples illustrate the principle of using domains for linking genotype and phenotype and for inferring the biological relevance of rare mutations in homologous genes. This process of informational aggregation may also lead to the discovery of the functional roles of domains not previously associated with oncogenesis, particularly in cases where the frequency of mutations in each of the domains separately is below the recurrence threshold but rises above the threshold when the multiple domain instances are equivalenced. For example, DUF3497, which is found in members of the G-protein-coupled receptor 2 family, has not been previously described as being involved in cancer processes, but mutations in lung cancer and melanoma samples significantly cluster in a hotspot in this domain with a total of seven mutations observed in *BAI3* (R588P/Q), *ELTD1* (K132E/N), and *CELSR1* (T2124A) (Figure S7C). This hotspot, with recurrent mutations in mostly basic amino acids (six out of seven mutations in K and R), is tantalizing because it suggests that mutations in this ''domain of unknown function'' confer a selective, functional advantage to cancer cells.

We here analyze mutations across domains in a set of related genes with the aim of identifying recurrent mutations with functional relevance (positive hotspots). However, if passenger

mutations without functional relevance are aggregated across several genes, an approach based on homologous domains may incur the risk of detecting false positive hotspots compared to a gene-based approach. The detection of spurious domain hotspots could be exacerbated by mutation biases that alter amino acids disproportionately. For example, arginine is the most frequently altered amino acid in the majority of tumor types (Figure S1) as it has four codons containing CG dinucleotides, which are frequently subject to C→T transitions due to deamination of methylated cytosine to thymine. In several domains, such as the tetramerization (K_tetra) domain of potassium channel proteins (Table S1) and the zf-H2C2 2 domain of zinc finger proteins (Table 2, row 16), we identified significant hotspots where arginine mutations align across a large set of genes in the domain family. Although the frequency of such hotspots may be driven by the arginine mutation bias, the mutations themselves may nevertheless be functional.

Future work will aim to refine the analysis of mutations in domains and expand the scope of our analysis to other functional elements in genes. Our focus here was on somatic missense mutations, but this requirement may be relaxed to include germ-line mutations or other somatic alterations (e.g., truncating mutations and small in-frame insertions and deletions). Importantly, truncating mutations affecting a particular domain may not necessarily actually be located in the domain but upstream of it, so we excluded truncating mutations from this work. An additional extension of our work would be to implement a sliding window for peak detection of clusters of mutations in domain alignments. However, our own observations suggest that mutation hotspots are largely limited to single residues. Other types of regulatory protein motifs can be analyzed, including short linear motifs that guide protein phosphorylation by kinases, which have previously been shown to be enriched for cancer-associated mutations in some genes (Reimand and Bader, 2013; Reimand et al., 2013). Finally, assessment of the functional impact of mutations using structural information and evolutionary sequence conservation, for example, as applied in our mutation assessor method (Reva et al., 2011), and evolutionary residue-residue couplings derived from correlated mutations in protein family alignments (Marks et al., 2011, 2012) can be incorporated to provide additional insight into the potential role of mutations in cancer.

As more data become available, integrative approaches combining functional evidence across multiple scales such as genes, domains, and signaling pathways will be needed to improve the computational pipelines for variant function prediction. To make the results of our analysis directly useful to the community at large, we have made all findings available through an interactive web service (http://www.mutationaligner.org), which is connected to our cBioPortal database for cancer genomics data (http://www.cbioportal.org) through bidirectional links. The MutationAligner web resource will be periodically updated as mutation data on genomically profiled tumor samples becomes available in the public domain.

EXPERIMENTAL PROCEDURES

Data Collection and Analysis

Detailed description of methods can be found in the Supplemental Experimental Procedures. Briefly, around 460,000 missense mutations from 5,496 exome-sequenced tumor-normal pairs of 22 different tumor types studied by the TGCA consortium were obtained from the cBioPortal (Cerami et al., 2012; Gao et al., 2013) in the format of TCGA level 3 variant data. Missense mutations were mapped to protein sequences and protein domains annotated by Pfam-A version 26 (Punta et al., 2012). Pfam-A domains were excluded from the analysis if (1) no missense mutations were present, (2) the Pfam-A expectancy score (e-value) was greater than $1e^{-5}$, or (3) the domain was only present as one instance in the human genome. To assess whether the mutation burden of the domain was larger than would be expected by chance, we (1) implemented a permutation test, which compared the observed mutation burden of the domain to the distribution of burdens generated by randomly distributing mutations across genes containing the domain; and (2) calculated a domain mutation enrichment score (Equation 1, Supplemental Experimental Procedures). To identify putative hotspots for mutations within domains, we used multiple sequence alignment of domain regions across protein families using BLOSUM80 as a scoring matrix. Mutations were tallied across samples and across domain-containing genes using the coordinates of the multiple sequence alignment. We used a binomial test, taking into account the length and total number of mutations observed in the domain, to generate a p value by comparing the number of mutations observed at that domain position to what would be observed by chance assuming a random distribution of mutations (Equations 2 and 3, Supplemental Experimental Procedures). We calculated an entropy score (S) based on Shannon information entropy to estimate how uniformly mutations are spread across domain-containing genes, where a high score indicates that multiple genes contribute to the observed mutations in the domain. The entropy score was normalized ($\overline{S}$) to the domain family size, with a maximum score of 1, signifying that mutation counts are the same for all genes (Equations 4 and 5, Supplemental Experimental Procedures). In total, 17,273 positions in the domain sequence alignments were analyzed based on the following criteria: (1) at least two mutations occurred at each position and (2) at least three-quarters of the domain alignments were non-gaps at each position (residues with alignment gaps in more than 75% of the sequences were excluded from the domain hotspot analysis). All p values were adjusted for multiple hypothesis testing using the stringent Bonferroni correction method.

SUPPLEMENTAL INFORMATION

Supplemental Information includes Supplemental Experimental Procedures, seven figures, and two tables and can be found with this article online at http://dx.doi.org/10.1016/j.cels.2015.08.014.

AUTHOR CONTRIBUTIONS

M.L.M. and E.R. designed analysis. N.P.G. designed and developed the website. M.L.M., E.R., N.P.G., B.A.A., A.K., J.G., G.C., N.S., and C.S. analyzed data. M.L.M. conceived and developed the concept. M.L.M. and C.S. managed the project. M.L.M., E.R., N.P.G., and C.S. wrote manuscript. All authors contributed to discussions and editing of the manuscript.

ACKNOWLEDGMENTS

We acknowledge C. Kandoth for technical assistance; C. Carmona-Fontaine, Debora S. Marks, and A. Hanrahan for helpful discussions; and V.A. Pedicord for helpful comments on the manuscript. This work was funded in part by the National Cancer Institute Cancer Genome Atlas grant (U24CA143840) and in part by Cancer Research UK (reference number C14303/A17197).

Received: November 20, 2014
Revised: July 5, 2015
Accepted: August 28, 2015
Published: September 23, 2015

REFERENCES

Adzhubei, I.A., Schmidt, S., Peshkin, L., Ramensky, V.E., Gerasimova, A., Bork, P., Kondrashov, A.S., and Sunyaev, S.R. (2010). A method and server for predicting damaging missense mutations. Nat. Methods 7, 248–249.

Alexandrov, L.B., Nik-Zainal, S., Wedge, D.C., Aparicio, S.A.J.R., Behjati, S., Biankin, A.V., Bignell, G.R., Bolli, N., Borg, A., Børresen-Dale, A.-L., et al.; Australian Pancreatic Cancer Genome Initiative; ICGC Breast Cancer Consortium; ICGC MMML-Seq Consortium; ICGC PedBrain (2013). Signatures of mutational processes in human cancer. Nature *500*, 415–421.

Bell, D., Berchuck, A., Birrer, M., Chien, J., Cramer, D.W., Dao, F., Dhir, R., DiSaia, P., Gabra, H., Glenn, P., et al.; Cancer Genome Atlas Research Network (2011). Integrated genomic analyses of ovarian carcinoma. Nature *474*, 609–615.

Betts, M.J., Lu, Q., Jiang, Y., Drusko, A., Wichmann, O., Utz, M., Valtierra-Gutiérrez, I.A., Schlesner, M., Jaeger, N., Jones, D.T., et al. (2015). Mechismo: predicting the mechanistic impact of mutations and modifications on molecular interactions. Nucleic Acids Res. *43*, e10.

Bromberg, Y., Yachdav, G., and Rost, B. (2008). SNAP predicts effect of mutations on protein function. Bioinformatics *24*, 2397–2398.

Cancer Genome Atlas Network (2012). Comprehensive molecular characterization of human colon and rectal cancer. Nature *487*, 330–337.

Carlsson, P., and Mahlapuu, M. (2002). Forkhead transcription factors: key players in development and metabolism. Dev. Biol. *250*, 1–23.

Cerami, E., Demir, E., Schultz, N., Taylor, B.S., and Sander, C. (2010). Automated network analysis identifies core pathways in glioblastoma. PLoS ONE *5*, e8918.

Cerami, E., Gao, J., Dogrusoz, U., Gross, B.E., Sumer, S.O., Aksoy, B.A., Jacobsen, A., Byrne, C.J., Heuer, M.L., Larsson, E., et al. (2012). The cBio cancer genomics portal: an open platform for exploring multidimensional cancer genomics data. Cancer Discov. *2*, 401–404.

Cerchietti, L.C., Hatzi, K., Caldas-Lopes, E., Yang, S.N., Figueroa, M.E., Morin, R.D., Hirst, M., Mendez, L., Shaknovich, R., Cole, P.A., et al. (2010). BCL6 repression of EP300 in human diffuse large B cell lymphoma cells provides a basis for rational combinatorial therapy. J. Clin. Invest. *120*, 4569–4582.

Chothia, C., Gough, J., Vogel, C., and Teichmann, S.A. (2003). Evolution of the protein repertoire. Science *300*, 1701–1703.

Chu, Y.P., Chang, C.H., Shiu, J.H., Chang, Y.T., Chen, C.Y., and Chuang, W.J. (2011). Solution structure and backbone dynamics of the DNA-binding domain of FOXP1: insight into its domain swapping and DNA binding. Protein Sci. *20*, 908–924.

Ciriello, G., Cerami, E., Sander, C., and Schultz, N. (2012). Mutual exclusivity analysis identifies oncogenic network modules. Genome Res. *22*, 398–406.

Creighton, C.J., Morgan, M., Gunaratne, P.H., Wheeler, D.A., Gibbs, R.A., Gordon Robertson, A., Chu, A., Beroukhim, R., Cibulskis, K., Signoretti, S., et al.; Cancer Genome Atlas Research Network (2013). Comprehensive molecular characterization of clear cell renal cell carcinoma. Nature *499*, 43–49.

Dees, N.D., Zhang, Q., Kandoth, C., Wendl, M.C., Schierding, W., Koboldt, D.C., Mooney, T.B., Callaway, M.B., Dooling, D., Mardis, E.R., et al. (2012). MuSiC: identifying mutational significance in cancer genomes. Genome Res. *22*, 1589–1598.

Dibb, N.J., Dilworth, S.M., and Mol, C.D. (2004). Switching on kinases: oncogenic activation of BRAF and the PDGFR family. Nat. Rev. Cancer *4*, 718–727.

Ding, L., Getz, G., Wheeler, D.A., Mardis, E.R., McLellan, M.D., Cibulskis, K., Sougnez, C., Greulich, H., Muzny, D.M., Morgan, M.B., et al. (2008). Somatic mutations affect key pathways in lung adenocarcinoma. Nature *455*, 1069–1075.

Fleming, N.I., Jorissen, R.N., Mouradov, D., Christie, M., Sakthianandeswaren, A., Palmieri, M., Day, F., Li, S., Tsui, C., Lipton, L., et al. (2013). SMAD2, SMAD3 and SMAD4 mutations in colorectal cancer. Cancer Res. *73*, 725–735.

Gao, J., Aksoy, B.A., Dogrusoz, U., Dresdner, G., Gross, B., Sumer, S.O., Sun, Y., Jacobsen, A., Sinha, R., Larsson, E., et al. (2013). Integrative analysis of complex cancer genomics and clinical profiles using the cBioPortal. Sci. Signal. *6*, pl1.

Garraway, L.A., and Lander, E.S. (2013). Lessons from the cancer genome. Cell *153*, 17–37.

Gonzalez-Perez, A., and Lopez-Bigas, N. (2012). Functional impact bias reveals cancer drivers. Nucleic Acids Res. *40*, e169.

Göthel, S.F., and Marahiel, M.A. (1999). Peptidyl-prolyl cis-trans isomerases, a superfamily of ubiquitous folding catalysts. Cell. Mol. Life Sci. *55*, 423–436.

Greenman, C., Stephens, P., Smith, R., Dalgliesh, G.L., Hunter, C., Bignell, G., Davies, H., Teague, J., Butler, A., Stevens, C., et al. (2007). Patterns of somatic mutation in human cancer genomes. Nature *446*, 153–158.

Greulich, H., Kaplan, B., Mertins, P., Chen, T.-H., Tanaka, K.E., Yun, C.-H., Zhang, X., Lee, S.-H., Cho, J., Ambrogio, L., et al. (2012). Functional analysis of receptor tyrosine kinase mutations in lung cancer identifies oncogenic extracellular domain mutations of ERBB2. Proc. Natl. Acad. Sci. USA *109*, 14476–14481.

Hammerman, P.S., Lawrence, M.S., Voet, D., Jing, R., Cibulskis, K., Sivachenko, A., Stojanov, P., McKenna, A., Lander, E.S., Gabriel, S., et al.; Cancer Genome Atlas Research Network (2012). Comprehensive genomic characterization of squamous cell lung cancers. Nature *489*, 519–525.

Hanahan, D., and Weinberg, R.A. (2011). Hallmarks of cancer: the next generation. Cell *144*, 646–674.

Hofree, M., Shen, J.P., Carter, H., Gross, A., and Ideker, T. (2013). Network-based stratification of tumor mutations. Nat. Methods *10*, 1108–1115.

Holm, L., and Sander, C. (1996). Mapping the protein universe. Science *273*, 595–603.

Jaiswal, B.S., Kljavin, N.M., Stawiski, E.W., Chan, E., Parikh, C., Durinck, S., Chaudhuri, S., Pujara, K., Guillory, J., Edgar, K.A., et al. (2013). Oncogenic ERBB3 mutations in human cancers. Cancer Cell *23*, 603–617.

Kandoth, C., Schultz, N., Cherniack, A.D., Akbani, R., Liu, Y., Shen, H., Robertson, A.G., Pashtan, I., Shen, R., Benz, C.C., et al.; Cancer Genome Atlas Research Network (2013). Integrated genomic characterization of endometrial carcinoma. Nature *497*, 67–73.

Koboldt, D.C., Fulton, R.S., McLellan, M.D., Schmidt, H., Kalicki-Veizer, J., McMichael, J.F., Fulton, L.L., Dooling, D.J., Ding, L., Mardis, E.R., et al.; Cancer Genome Atlas Network (2012). Comprehensive molecular portraits of human breast tumours. Nature *490*, 61–70.

Lawrence, M.S., Stojanov, P., Polak, P., Kryukov, G.V., Cibulskis, K., Sivachenko, A., Carter, S.L., Stewart, C., Mermel, C.H., Roberts, S.A., et al. (2013). Mutational heterogeneity in cancer and the search for new cancer-associated genes. Nature *499*, 214–218.

Lawrence, M.S., Stojanov, P., Mermel, C.H., Robinson, J.T., Garraway, L.A., Golub, T.R., Meyerson, M., Gabriel, S.B., Lander, E.S., and Getz, G. (2014). Discovery and saturation analysis of cancer genes across 21 tumour types. Nature *505*, 495–501.

Lee, J.C., Vivanco, I., Beroukhim, R., Huang, J.H.Y., Feng, W.L., DeBiasi, R.M., Yoshimoto, K., King, J.C., Nghiemphu, P., Yuza, Y., et al. (2006). Epidermal growth factor receptor activation in glioblastoma through novel missense mutations in the extracellular domain. PLoS Med. *3*, e485.

Liu, X., Wang, L., Zhao, K., Thompson, P.R., Hwang, Y., Marmorstein, R., and Cole, P.A. (2008). The structural basis of protein acetylation by the p300/CBP transcriptional coactivator. Nature *451*, 846–850.

Lohr, J.G., Stojanov, P., Lawrence, M.S., Auclair, D., Chapuy, B., Sougnez, C., Cruz-Gordillo, P., Knoechel, B., Asmann, Y.W., Slager, S.L., et al. (2012). Discovery and prioritization of somatic mutations in diffuse large B-cell lymphoma (DLBCL) by whole-exome sequencing. Proc. Natl. Acad. Sci. USA *109*, 3879–3884.

Marks, D.S., Colwell, L.J., Sheridan, R., Hopf, T.A., Pagnani, A., Zecchina, R., and Sander, C. (2011). Protein 3D structure computed from evolutionary sequence variation. PLoS ONE *6*, e28766.

Marks, D.S., Hopf, T.A., and Sander, C. (2012). Protein structure prediction from sequence variation. Nat. Biotechnol. *30*, 1072–1080.

McLendon, R., Friedman, A., Bigner, D., Van Meir, E.G., Brat, D.J.M., Mastrogianakis, G., Olson, J.J., Mikkelsen, T., Lehman, N., Aldape, K., et al.; Cancer Genome Atlas Research Network (2008). Comprehensive genomic characterization defines human glioblastoma genes and core pathways. Nature *455*, 1061–1068.

Morin, R.D., Mendez-Lago, M., Mungall, A.J., Goya, R., Mungall, K.L., Corbett, R.D., Johnson, N.A., Severson, T.M., Chiu, R., Field, M., et al. (2011). Frequent

mutation of histone-modifying genes in non-Hodgkin lymphoma. Nature *476*, 298–303.

Nehrt, N.L., Peterson, T.A., Park, D., and Kann, M.G. (2012). Domain landscapes of somatic mutations in cancer. BMC Genomics *13* (*Suppl 4*), S9.

Ng, P.C., and Henikoff, S. (2003). SIFT: Predicting amino acid changes that affect protein function. Nucleic Acids Res. *31*, 3812–3814.

Ohtaki, N., Yamaguchi, A., Goi, T., Fukaya, T., Takeuchi, K., Katayama, K., Hirose, K., and Urano, T. (2001). Somatic alterations of the DPC4 and Madr2 genes in colorectal cancers and relationship to metastasis. Int. J. Oncol. *18*, 265–270.

Pasqualucci, L., Dominguez-Sola, D., Chiarenza, A., Fabbri, G., Grunn, A., Trifonov, V., Kasper, L.H., Lerach, S., Tang, H., Ma, J., et al. (2011). Inactivating mutations of acetyltransferase genes in B-cell lymphoma. Nature *471*, 189–195.

Peifer, M., Fernández-Cuesta, L., Sos, M.L., George, J., Seidel, D., Kasper, L.H., Plenker, D., Leenders, F., Sun, R., Zander, T., et al. (2012). Integrative genome analyses identify key somatic driver mutations of small-cell lung cancer. Nat. Genet. *44*, 1104–1110.

Peterson, T.A., Adadey, A., Santana-Cruz, I., Sun, Y., Winder, A., and Kann, M.G. (2010). DMDM: domain mapping of disease mutations. Bioinformatics *26*, 2458–2459.

Peterson, T.A., Nehrt, N.L., Park, D., and Kann, M.G. (2012). Incorporating molecular and functional context into the analysis and prioritization of human variants associated with cancer. J. Am. Med. Inform. Assoc. *19*, 275–283.

Punta, M., Coggill, P.C., Eberhardt, R.Y., Mistry, J., Tate, J., Boursnell, C., Pang, N., Forslund, K., Ceric, G., Clements, J., et al. (2012). The Pfam protein families database. Nucleic Acids Res. *40*, D290–D301.

Reimand, J., and Bader, G.D. (2013). Systematic analysis of somatic mutations in phosphorylation signaling predicts novel cancer drivers. Mol. Syst. Biol. *9*, 637.

Reimand, J., Wagih, O., and Bader, G.D. (2013). The mutational landscape of phosphorylation signaling in cancer. Sci. Rep. *3*, 2651.

Reva, B., Antipin, Y., and Sander, C. (2011). Predicting the functional impact of protein mutations: application to cancer genomics. Nucleic Acids Res. *39*, e118.

Shi, Y., Hata, A., Lo, R.S., Massagué, J., and Pavletich, N.P. (1997). A structural basis for mutational inactivation of the tumour suppressor Smad4. Nature *388*, 87–93.

Stroud, J.C., Wu, Y., Bates, D.L., Han, A., Nowick, K., Paabo, S., Tong, H., and Chen, L. (2006). Structure of the forkhead domain of FOXP2 bound to DNA. Structure *14*, 159–166.

Torkamani, A., and Schork, N.J. (2009). Identification of rare cancer driver mutations by network reconstruction. Genome Res. *19*, 1570–1578.

Tsai, K.L., Huang, C.Y., Chang, C.H., Sun, Y.J., Chuang, W.J., and Hsiao, C.D. (2006). Crystal structure of the human FOXK1a-DNA complex and its implications on the diverse binding specificity of winged helix/forkhead proteins. J. Biol. Chem. *281*, 17400–17409.

Wang, N.J., Sanborn, Z., Arnett, K.L., Bayston, L.J., Liao, W., Proby, C.M., Leigh, I.M., Collisson, E.A., Gordon, P.B., Jakkula, L., et al. (2011). Loss-of-function mutations in Notch receptors in cutaneous and lung squamous cell carcinoma. Proc. Natl. Acad. Sci. USA *108*, 17761–17766.

Weng, A.P., Ferrando, A.A., Lee, W., Morris, J.P., 4th, Silverman, L.B., Sanchez-Irizarry, C., Blacklow, S.C., Look, A.T., and Aster, J.C. (2004). Activating mutations of NOTCH1 in human T cell acute lymphoblastic leukemia. Science *306*, 269–271.

Wu, J.W., Hu, M., Chai, J., Seoane, J., Huse, M., Li, C., Rigotti, D.J., Kyin, S., Muir, T.W., Fairman, R., et al. (2001). Crystal structure of a phosphorylated Smad2. Recognition of phosphoserine by the MH2 domain and insights on Smad function in TGF-beta signaling. Mol. Cell *8*, 1277–1289.

Wu, Y., Borde, M., Heissmeyer, V., Feuerer, M., Lapan, A.D., Stroud, J.C., Bates, D.L., Guo, L., Han, A., Ziegler, S.F., et al. (2006). FOXP3 controls regulatory T cell function through cooperation with NFAT. Cell *126*, 375–387.

Wu, J.Y., Yu, C.J., Chang, Y.C., Yang, C.H., Shih, J.Y., and Yang, P.C. (2011). Effectiveness of tyrosine kinase inhibitors on "uncommon" epidermal growth factor receptor mutations of unknown clinical significance in non-small cell lung cancer. Clin. Cancer Res. *17*, 3812–3821.

Yang, F., Petsalaki, E., Rolland, T., Hill, D.E., Vidal, M., and Roth, F.P. (2015). Protein domain-level landscape of cancer-type-specific somatic mutations. PLoS Comput. Biol. *11*, e1004147.

Yue, P., Melamud, E., and Moult, J. (2006). SNPs3D: candidate gene and SNP selection for association studies. BMC Bioinformatics *7*, 166.

Yue, P., Forrest, W.F., Kaminker, J.S., Lohr, S., Zhang, Z., and Cavet, G. (2010). Inferring the functional effects of mutation through clusters of mutations in homologous proteins. Hum. Mutat. *31*, 264–271.